On the Local Structure of Liquid Gallium from EXAFS Studies

Armando H. Shinohara[1] , Kazuhiko Omote[2], Yoshio Waseda[2] and James M. Toguri[3]

[1] *Faculty of Mechanical Engineering, FEM-DEMA, C.P. 6122, 13081-970 Campinas, SP, Brazil*
[2] *Institute for Advanced Materials Processing, Tohoku University, Sendai 980-77, Japan*
[3] *Department of Metallurgy and Materials Science, University of Toronto, Toronto, Ontario M5S3E4, Canada*

(Received September 4, 1995; final form December 8, 1995)

ABSTRACT

The EXAFS technique has been applied for obtaining information on the local atomic arrangements in the near neighbor region of liquid gallium. The EXAFS data of liquid gallium at temperatures of 323 and 473 K can be well explained by considering four immediate neighbors and another four slightly more distant neighbors located so as to form a local structure around each atom. The present results can account for the first peak asymmetry of the radial distribution function obtained from X-ray diffraction studies.

1. INTRODUCTION

The local structure of liquid gallium has been extensively investigated by both X-ray /1-4/ and neutron /5-8/ diffraction techniques. The first peak in the radial distribution function (RDF) of liquid gallium is found to be asymmetrical. To account for this observation, it has been proposed that a local ordinary structure occurs in liquid gallium /9/. However, the origin of this structural feature has not been identified. It is now well-recognized that with the EXAFS method it is possible to obtain the local structure of materials including non-crystalline systems /10/. The EXAFS analysis for liquid gallium /11/ suggests that one nearest neighbor is at 0.244 nm and another two are located at 0.268 nm. These results do not agree with those of the diffraction data which indicate that the nearest neighbor atoms are located at 0.282 nm with a coordination number of about 9-10 /7/. To clarify these reported results, EXAFS studies were performed on liquid gallium at 323 and 473 K to characterize its local structure.

2. EXPERIMENTAL

EXAFS measurements were made by an in-house apparatus. Since details of this equipment have been described elsewhere /12/, only some characteristic features are given in this report. The principal arrangement of the spectrometer is shown in Fig. 1. A rotating anode type high power X-ray generator (Rigaku RU-7AV) with a Johanson-type monochromator crystal was used for obtaining a high-intensity photon flux. The maximum power of the X-ray generator was 40 kV and 450 mA while the effective size of the source was 10 × 0.05 mm^2 at a take-off angle of 6°. The goniometer was moved by three pulse motors. One (PM1) was to move three points, the X-ray source, the monochromator crystal and the receiving slit, on a Rowland circle of 640 mm diameter. The other two (PM2 and PM3) were also to turn the X-ray source and the parts containing the sample and detectors which are parallel to the optical axis. The diffraction angle of the

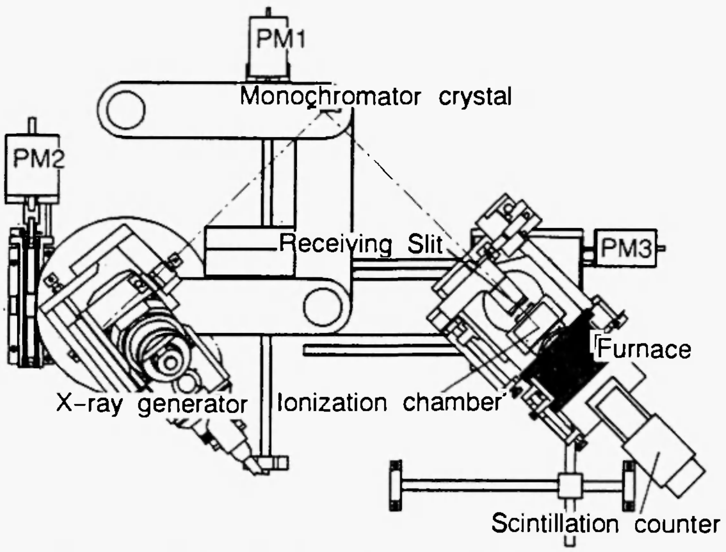

Fig. 1: The principal arrangement of the EXAFS apparatus for high-temperature molten materials.

X-rays can be varied from 17° to 60° by the rotation of the monochromator crystal.

The absorption spectrum of the gallium *K* edge (10368 eV) was obtained using a molybdenum target and a Ge (400) monochromator crystal. The measurements were carried out in the transmission mode. High purity gallium of 99.999% (Nilaco Corporation) was used in this work. A sample of 15 μm in thickness was sandwiched between two quartz planes each of 100 μm thickness. A schematic diagram of this cell system is shown in Fig. 2. This cell system was heated by a tungsten wound furnace under an argon atmosphere.

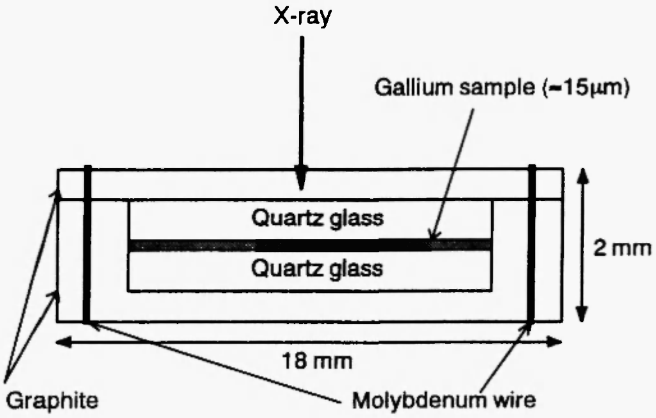

Fig. 2: A sample cell used to keep liquid gallium for EXAFS measurement in the transmission mode. Sample was sandwiched between two quartz plates and held in position by two plates of graphite fixed with molybdenum wire (MW).

The technique of EXAFS analyses has been applied to structural studies of various substances and its procedure is now well established /10/. Thus, only the essential points employed in this work are given below. The oscillatory part, $\chi(k)$, of the X-ray absorption coefficient for a particular element beyond its absorption edge may be given by the expression,

$$\chi(k) = \frac{m}{4\pi h^2 k} \sum_j \frac{N_j}{r_j^2} t_j(k) \exp(-2r_j/\lambda_e) \sin(2kr_j + \delta_j(k)) \exp(-2k^2\sigma_j^2), \qquad (1)$$

where h is Planck's constant, k the wavevector of the photoelectron, λ_e the mean free path of the photoelectron, and r_j, σ_j^2 and N_j are the radial distance, mean square fluctuation and coordination number of the j-type atoms from an absorbing atom, respectively. $t_j(k)$ denotes the back scattering amplitude encountered by the photoelectrons, $\delta_j(k)$ the phase shift required to account for the potentials arising from both a central absorbing atom and a neighboring atom (back scattering). A Fourier transform of the EXAFS spectrum,

$$\phi_n(r) = \frac{1}{\sqrt{2\pi}} \int_0^\infty k^n \chi(k) \exp(-2ikr) W(k)\, dk, \qquad (2)$$

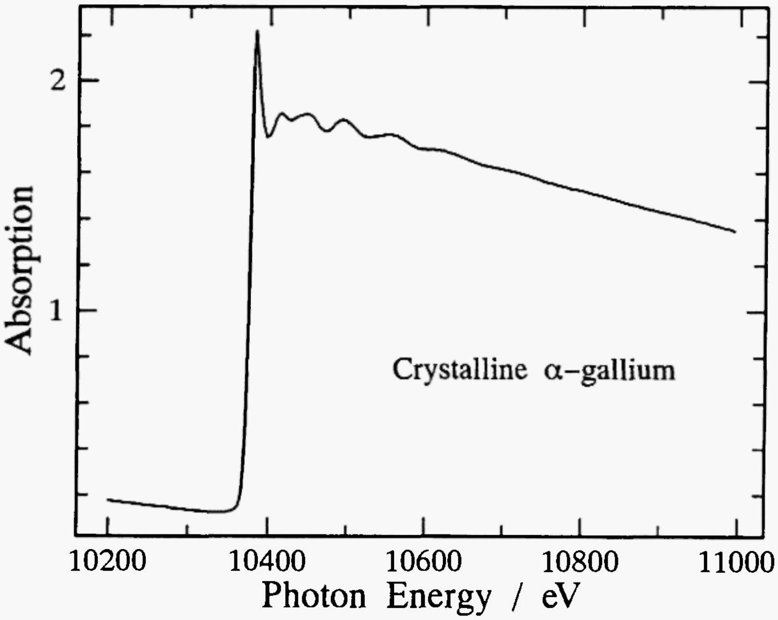

Fig. 3: Gallium K-edge absorption spectrum of crystalline α-gallium of 15 μm in thickness at room temperature.

provides information about the distribution of neighboring atoms for a central absorbing atom. $W(k)$ is a window function that is chosen to minimize the spurious ripples in $\phi_n(r)$ due to a finite range of $\chi(k)$. Referring to the EXAFS results for various substances, $n = 3$ was employed in this work.

3. RESULTS AND DISCUSSION

The recent availability of a high intensity X-ray source and the Fourier transformation analysis proposed by Stern *et al.* /13/ have led to the development of the EXAFS method as a useful tool for obtaining the local structure around an X-ray absorbing atom. This resulted because the structural data in the higher wave vector region can be obtained with ease compared to diffraction experiments /14/. It may be worth noting that the wave vector of the photoelectron k corresponds to twice the momentum transfer of the diffraction experiments $Q = \left(\frac{4\pi \sin\theta}{\lambda}\right)$, where the θ is half of the scattering angle and λ is the wavelength of the incident waves. This allows a higher resolution of the atomic correlations in the near neighbor region, although information of the long-range ordering is frequently excluded. The near neighbor structure of crystalline α-gallium was investigated in order to determine a few of the unknown physical parameters such as the mean-free path and the energy shift of the photoelectron required for the EXAFS analysis as well as the usefulness of the generalized computer program /15/. It is helpful to note that the coordination number of the nearest neighbors of crystalline α-gallium is seven; where one atom is located closer at a distance of 0.248 nm, and another six atoms are distributed at distances of 0.269 nm, 0.273 nm and 0.279 nm as given in Table 1.

Figure 3 shows the measured absorption spectrum of a thin foil of crystalline α-gallium 15 μm in thickness at room temperature. Figure 4 (a) gives the magnitude of the Fourier transform of the EXAFS obtained by the common procedure. The first peak corresponds to the atomic distribution in the near neighbor region around an absorbing atom. The two small peaks denoted by arrows 2nd and 3rd are attributed to the longer range atomic correlation in crystalline α-gallium. To extract the unknown parameters, the main peak was selected by Fourier filtering and its inverse Fourier transformation was made so as to reproduce the EXAFS spectrum. Here, the curve fitting has been conducted by taking into account that the local structure of crystalline α-gallium consists of two

Table 1
Local structural parameters of liquid gallium obtained by EXAFS

	Interatomic distance (nm)		Mean square fluctuation (nm^2)	Coordination number	
α-gallium	0.248	0.248	-	1	1
	0.269	0.274	-	2	6
	0.273		-	2	
	0.279		-	2	
β-gallium	0.268	0.273	-	2	4
	0.277		-	2	
	0.287	0.290	-	2	4
	0.292		-	2	
Liquid gallium 323 K	0.270	0.280	$(0.013)^2$	4.0	7.8
	0.289		$(0.021)^2$	3.8	
473 K	0.265	0.279	$(0.014)^2$	3.9	7.6
	0.292		$(0.022)^2$	3.7	

correlations where one atom is located at 0.248 nm and the other six are distributed at an average distance of 0.274 nm. As can be easily seen from the results of Fig. 4 (b), the measured EXAFS spectrum is found to be reproduced well by considering the local structure of crystalline α-gallium. The values of the mean-free path and the energy shift of the photoelectron determined in this process for crystalline α-gallium are employed in data processing of the local structure in liquid gallium. Such assumptions may safely be accepted because only short range ordering in the near neighbor region is significant after melting /10,14/.

Figure 5 shows the absorption spectrum of liquid gallium at temperatures of 323 and 473 K. In both cases, the oscillations are clearly observed suggesting that a considerable fraction of a certain local atomic correlation remains in liquid gallium. This supports and gives a higher reliability to the evaluation of the near neighbor structure around an absorbing atom.

According to the results obtained by X-ray and neutron diffraction techniques, the interatomic distance and its coordination number of nearest neighbors in liquid gallium at 323 K are 0.282 nm and 8.8, respectively /7/. Based on this data, the EXAFS spectrum was evaluated. However, the agreement between the calculated and measured EXAFS data is far from complete, as shown by Fig. 6. The discrepancy is not improved by changing the values of the interatomic distance or the coordination number. For this reason, further calculations were made by introducing a local atomic arrangement in the near neighbor region in liquid gallium consisting of two different correlations as observed in crystalline α-gallium. The results are given in Fig. 7 and the resultant structural parameters are listed in Table 1. As shown in Fig. 7, the agreement between the experimental and calculated EXAFS appears to be satisfactory in the two cases. As Table 1 clearly indicates, the local atomic arrangements in the near neighbor region of liquid gallium can be explained by a model in which each atom has approximately four immediate neighbors and another set of four neighbors located at a slightly longer distance. It is also worth mentioning that this local structural feature of liquid gallium is no closer to the crystalline α-gallium data than the crystalline β-gallium (high pressure phase) as shown in Table 1. When temperature increases, the

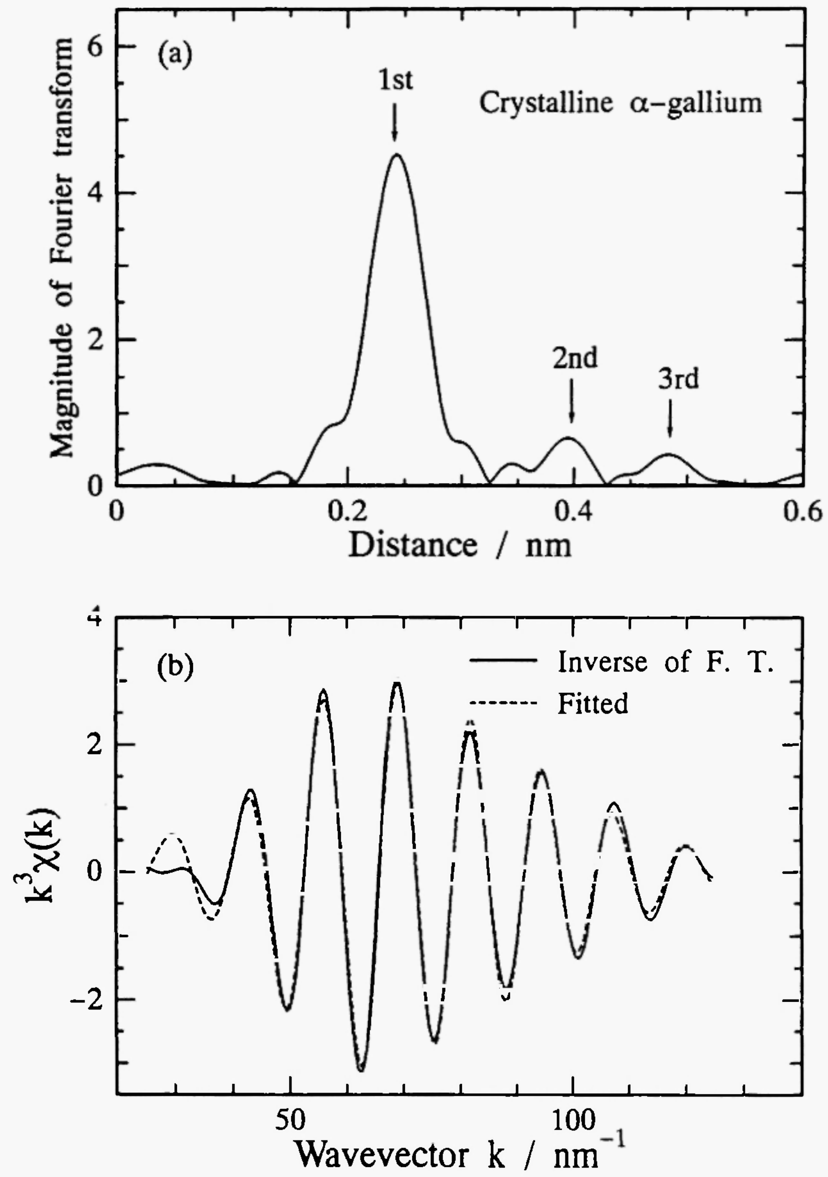

Fig. 4: (a) Magnitude of the Fourier transform of the EXAFS spectrum of crystalline α-gallium. (b) EXAFS spectra related to the nearest neighbor atoms; obtained by Fourier filtering technique (solid line) and simulated by using the local structural data of crystalline α-gallium (broken line).

atomic vibration is expected to contribute to changes in the structural features of liquids. However, for liquid gallium in the temperature range presently investigated, it is not too significant.

In conclusion, the local structure of liquid gallium can be accounted for by considering two correlations of four immediate neighbors and another four neighbors at a slightly more distant position. This characteristic feature represents a possible answer to the question about the first peak asymmetry of the radial distribution function obtained by X-ray and neutron diffraction. It would also be interesting to extend the EXAFS method to estimate the local structure in other liquid metals in order to obtain further details of their atomic structure.

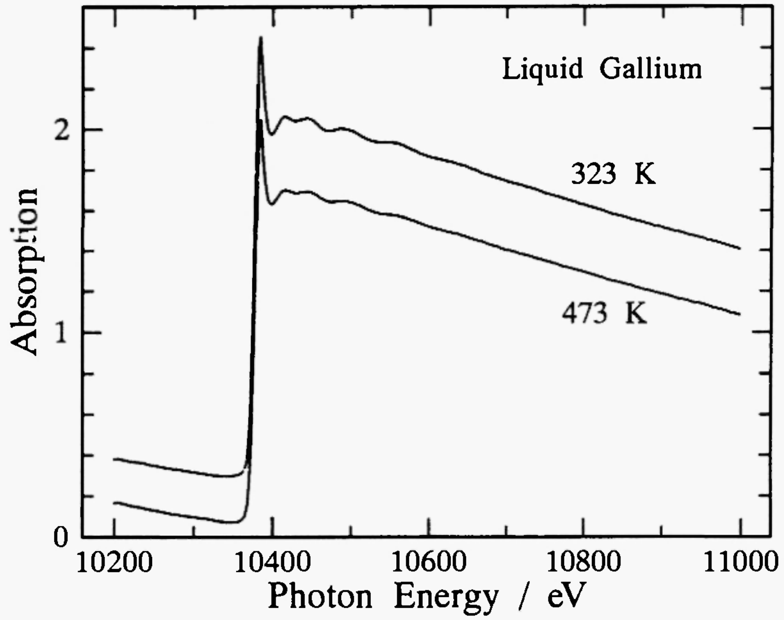

Fig. 5: Gallium K-edge absorption spectra of liquid gallium at 323 and 473 K.

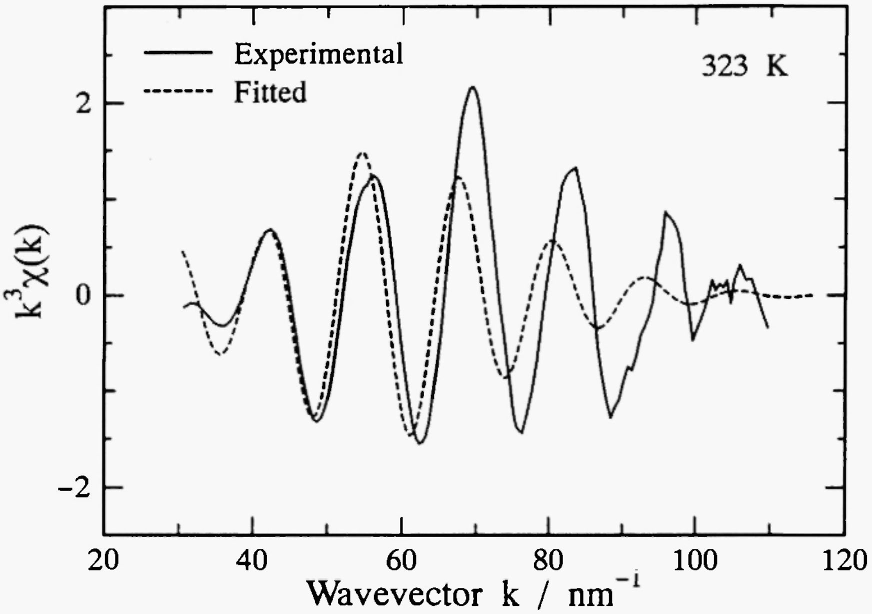

Fig. 6: Experimental EXAFS spectrum of liquid gallium at 323 K (solid line) together with simulated spectrum using the local structural data obtained by neutron diffraction (broken line).

ACKNOWLEDGEMENTS

The authors are grateful for the continuous support and encouragement of Dr. S. Kimura, National Institute for Inorganic Materials, and Professor K. Terashima, Shonan Institute of Technology.

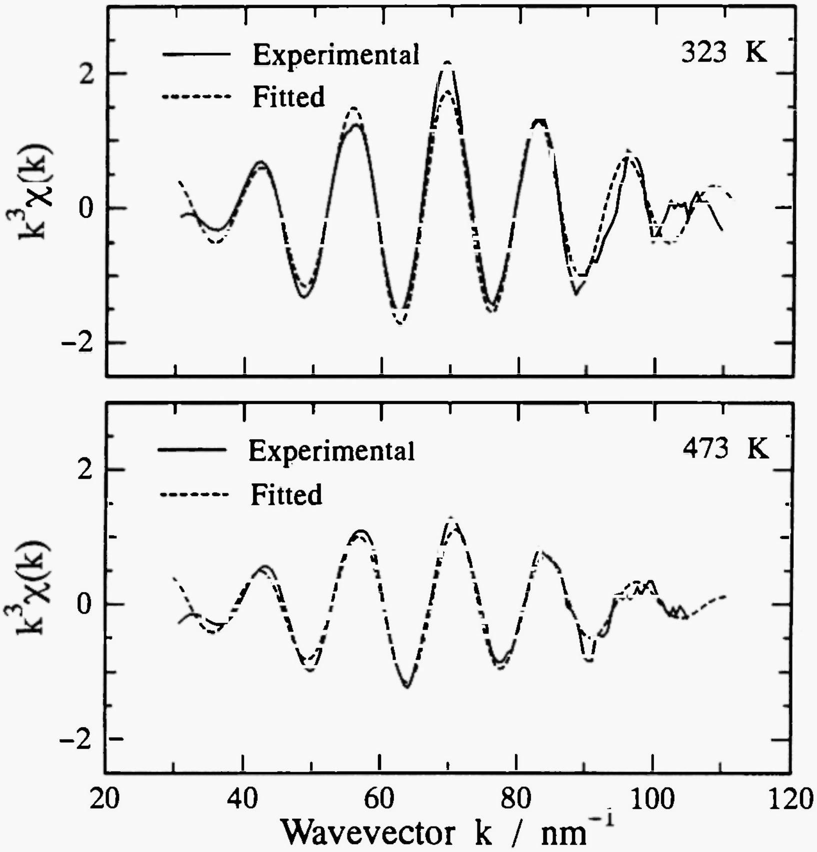

Fig. 7: Experimental EXAFS spectra of liquid gallium at 323 and 473 K (solid line) together with the spectra calculated by considering two different correlations in the nearest neighbors (broken line).

REFERENCES

1. S.E. Rodriguez and C.J. Pings, *J. Chem. Sol.*, 42 (7), 2435 (1964).
2. Y. Waseda and K. Suzuki, *Phys. Stat. Sol. (B)*, 49, 339 (1972).
3. A. Bizid, L. Bosio, H. Curien, A. Defrain and M. Dupont, *Phys. Stat. Sol. (A)*, **23**, 135 (1974).
4. A. Bizid, L. Bosio and R. Cortes, *J. Chim. Phys.*, 74 (7-8), 36 (1977).
5. P. Ascarelli, *Phys. Rev.*, **143** (1), 36 (1966).
6. K. Suzuki, M. Misawa and Y. Fukushima, *Trans. JIM*, 16, 297 (1975).
7. S. Takeda, S. Harada, S. Tamaki and Y. Waseda, *J. Phys. Soc. Jpn.*, **55** (10), 3437 (1986).
8. M.C. Bellissent-Funel, P. Chieux, D. Levesque and J.J. Weis, *Phys. Rev. A*, **39**, (12), 6310 (1989).
9. N.H. March, M. Parrinello and M.P. Tosi, *Phys. Chem. Liquids*, **5**, 39 (1976).
10. B.K. Teo, *EXAFS: Basic Principles and Data Analysis*, Springer-Verlag, Berlin, 1980.
11. B.R. Orton, *Inst. Phys. Conf. Ser.*, **101**, 77 (1989).
12. K. Omote, K. Tohji, Y. Waseda, A. Kiku and M. Funahashi, *Jpn. J. Appl. Phys.*, **32** (32-2), 267 (1992).
13. E.A. Stern, D.E. Sayers and F.W. Lytle, *Phys. Rev. Lett.*, **11**, 4836 (1975).
14. D.C. Koningsberger and R. Prins, *X-Ray Absorption: Principles, Applications, Techniques of EXAFS, SEXAFS, and XANES*, John Wiley & Sons, New York, 1988.
15. A.G. Mackale, B.W. Veal, A.P. Paulikas, S.K. Chain and G.S. Knapp, *J. Am. Chem. Soc.*, **110**, 3763 (1988).